

The Influence of Trifluoromethyl Groups on the Miscibility of Fluorinated Alcohols with Water: A Molecular Dynamics Simulation Study of 1,1,1-Trifluoropropan-2-ol in Aqueous Solution

Marco Fioroni,^{*,†} Klaus Burger,[‡] Alan E. Mark,[§] and Danilo Roccatano[#]

Department Chemical Engineering, Eindhoven University of Technology, Helix Building SKA, STW 4.34, P.O. Box 513, 5600 MB Eindhoven, The Netherlands, Fakultät für Chemie und Mineralogie, Institut für Organische Chemie, Johannisallee 29, 04103 Leipzig, Germany, Groningen Biomolecular Sciences and Biotechnology Institute (GBB), Department of Biophysical Chemistry, University of Groningen, Nijenborgh 4, 9747 AG Groningen, The Netherlands, and Dipartimento di Chimica, Ingegneria Chimica e Materiali, Università degli studi, v. Vetoio, 67010 L'Aquila, Italy

Received: May 7, 2002; In Final Form: December 3, 2002

1,1,1-Trifluoro-propan-2-ol (TFIP) alcohol has been used to study the influence of trifluoromethyl groups (CF₃) on the physicochemical properties of fluorinated organic molecules. TFIP contains both a CF₃ and a methyl (CH₃) group. An atomistic study of TFIP thus can provide insight into the behavior of the two groups in water. First, an all-atom model of TFIP was parametrized to reproduce the experimental density, pressure, and enthalpy of vaporization of the pure racemic liquid at 298 K. Mixtures of TFIP with water were then simulated at 298 K, and the structural, thermodynamic, and kinetic properties obtained were compared with the available experimental data. The structure of the hydration shell of the CF₃ group was found to be concentration-dependent. At concentrations at which TFIP and water are miscible, the organization of water around the CF₃ groups was similar to that found around the CH₃ groups. At concentrations at which TFIP and water are not miscible, the water around the CF₃ group was highly disordered. The structure of the water cage around the CH₃ groups was found to be similar for all of the water concentrations. This difference in organization of the hydration shell around the CF₃ and CH₃ groups may play a key role in determining the unusual miscibility behavior of TFIP as compared with other fluorinated compounds such as 2,2,2-trifluoroethanol and 1,1,1,3,3,3-hexafluoropropan-2-ol.

1. Introduction

The use of fluorinated compounds in medicinal and biological chemistry¹ is an active and growing field of research.^{2,3} For example, the presence of trifluoromethyl groups in small bioactive molecules will often improve pharmacological profiles.^{2,3} This effect has been related to the hydrophobic characteristics of the CF₃ group. Studies have shown a possible correlation between the hydrophobic properties of the CF₃ and CH₃ groups and their distance from any hydrophilic groups (such as OH) present in the molecule.^{4,5} However, no general rules have been established to define the relative hydrophobicity of CF₃ and CH₃ groups. Fluorinated alcohols are very good models to investigate this phenomenon. Experimental⁶ and theoretical^{7,8} studies of mixtures of 2,2,2-trifluoroethanol (TFE) and 1,1,1,3,3,3-hexafluoropropan-2-ol (HFIP) with water suggest a strong tendency for these alcohols to aggregate. This “clustering” is the result of the interactions between the CF₃ groups as they minimize their contact with water and of the hydrogen-bond network formed among the alcohol molecules. Experimental data suggest that the tendency for TFIP to cluster in aqueous solution is low.⁹ The presence of both CF₃ and CH₃ groups in

the same molecule has been claimed as a possible explanation for this observation.⁹ In fact, fluorocarbons and hydrocarbons have low mutual affinities. For example,¹⁰ mixtures of fluoroheptane and heptane deviate considerably from ideality, being only partially miscible at room temperature. Furthermore in aqueous solution, fluorocarbons and hydrocarbon surfactants form two distinct classes of micelles: one rich in the hydrocarbon surfactant and the other rich in the fluorocarbon.^{11,12} The strength of the dispersion forces between the CF₃ and CH₃ groups is believed to be one of the main reasons for this behavior.¹³ In TFIP, the presence of both CH₃ and CF₃ groups induces a related behavior, the partial miscibility of TFIP with water for a range of molar fractions. As a possible explanation of this phenomena, it has been claimed that the solvation shells around the CF₃ and CH₃ groups have different properties.^{9,14,15} In fact, the different nature of the interaction between water molecules and these two groups could account for the different degrees of association in the mixtures at different concentrations. For this reason, TFIP is a good model to investigate, at a molecular level, the nature of the hydrophobic effect of both CH₃ and CF₃. Insight onto the nature of this complex phenomenon can be obtained by an atomistic description based on simplified molecular models. Molecular dynamics (MD) simulations have already been used to provide insight into the thermodynamic and structural characteristics of other fluorinated solvents.^{7,8,16,17} Recent models of TFE⁷ and HFIP⁸ alcohols have been parametrized to reproduce thermodynamic properties of

* To whom correspondence should be addressed. Fax: +31-40-2455054. Electronic mail: M.Fioroni@tue.nl.

† Eindhoven University of Technology.

‡ Institut für Organische Chemie. Electronic mail: burger@organik.chemie.uni-leipzig.de.

§ University of Groningen. Electronic mail: mark@chem.rug.nl.

Università degli studi. Electronic mail: roccata@caspur.it.

the pure liquid and of water mixtures. A MD model of TFIP has been previously proposed by Kinugawa and Nakanishi¹⁸ and used to investigate the hydration of this solvent. The model was parametrized by fitting to quantum-mechanically (QM) derived interatomic potentials. Internal degrees of freedom were neglected in the simulations. The model reproduced the experimental hydration free energy of TFIP. However, in addition to alcohol–water interactions, correct alcohol–alcohol interactions are essential to determine the solubility of this alcohol. To our knowledge, no other TFIP model for MD simulation studies of TFIP have appeared in the literature.

In this paper, we propose a new model for TFIP and use this model to simulate water mixtures of this solvent at different molar fractions from 0 to 1. The aim of this study was to analyze the structural and dynamical behavior of water molecules around both the CF₃ and CH₃ groups present in TFIP. In addition, a comparison of the structural properties of TFIP with the structural properties of neat TFE or HFIP and related aqueous mixtures is also presented. The TFIP model, in the racemic form, was parametrized to reproduce the density, pressure, and vaporization enthalpy of the pure liquid at 298 K.

In developing this model for TFIP, the primary aim was to obtain a model compatible with an existing force field, in this case the GROMOS96¹⁹ force field for proteins together with the simple point charge model (SPC) for water developed by Berendsen and co-workers.²⁰ This was done in a similar manner as that used previously for other fluorinated solvents.^{7,8} The model is nonpolarizable in line with the GROMOS96 force field. In contrast to the GROMOS96 force field, however, hydrogens attached to the carbon atoms were treated explicitly. The model has been designed to be suitable for studying the conformational properties of peptides in water/TFIP mixtures.

The physicochemical properties of the optimized model were validated by comparison to a range of other experimental data. The thermodynamic and kinetic properties of mixtures with simple point charge model (SPC) for water²⁰ were determined and compared with experimental values. In particular, the organization of the water molecules around the CF₃ and the CH₃ groups was analyzed. The paper is organized as follows. In the Methods section, the procedure for the optimization of the TFIP interaction functions and the simulation protocol is described. In the first and second part of the Results, the structural and physicochemical properties of neat TFIP and TFIP/SPC water mixtures are reported and compared to those found for TFE and HFIP. In the Discussion, a possible explanation for the different thermodynamic properties of the CF₃ and CH₃ groups is discussed. Finally, in the Conclusions, a summary and outline of the work is given.

2. Methods

2.1. TFIP Force Field Parameters. The Gaussian 98 package²¹ was used to perform all of the ab initio calculations involving the TFIP molecules. Geometry optimization was performed using the 6-311++G** basis set at the self-consistent field (SCF) level. The same basis set was used for the calculation, at the Moller–Plesset second-order level (MP2), of the charge densities for the optimized structures.²² The equilibrium between different conformers as determined from ab initio calculations has been previously described by Schaal et al.²³ Bond lengths and angles in the different optimized conformers are very similar and were used to define the reference bond lengths and angles for the TFIP model (see Table 1). These are consistent with those previously used in the parametrization of TFE⁷ and HFIP.⁸ The atomic partial charges

TABLE 1: Parameters for the TFIP Model^a

atom type	$C_{i,i}^6$ (kJ mol ⁻¹ nm ⁶) × 10 ³	$C_{i,i}^{12}$ (kJ mol ⁻¹ nm ¹²) × 10 ⁶	q (e)
F	1.177 862	1.000 000	-0.240(0.01)
C _{CF₃}	2.340 624	3.374 569	0.600(0.17)
C _c	2.340 624	3.374 569	0.310(0.01)
C _{CH₃}	2.340 624	3.374 569	-0.320(0.08)
H _c	0.084 64	0.015 129	0.080(0.05)
H _{CH₃}	0.084 64	0.015 129	0.100(0.01)
O	2.261 954	0.945 000	-0.670(0.04)
H	0.000 00	0.000 000	0.420(0.04)

bond	length (nm)
C _{CF₃} -F	0.136
C _{CF₃} -C _c	0.153
C _{CH₃} -C _c	0.153
C _{CH₃} -H _{CH₃}	0.123
C _c -O	0.136
C _c -H _c	0.123
O-H	0.100

bond angle	θ_0 (deg)	K_θ (kJ mol ⁻¹ rad ⁻²)
C _{CF₃} -C _c -O	111.0	460.24
C _{CH₃} -C _c -O	111.0	460.24
C _{CF₃} -C _c -H _c	109.5	460.24
C _{CH₃} -C _c -H _c	109.5	460.24
C _{CF₃} -C _c -C _{CH₃}	111.0	460.24
F-C _{CF₃} -F	107.6	460.24
F-C _{CF₃} -C _c	111.4	460.24
C _c -O-H	109.5	397.48
O-C _c -H _c	109.5	397.48
H _{CH₃} -C _{CH₃} -H _{CH₃}	111.0	475.00
H _{CH₃} -C _{CH₃} -C _c	109.5	460.24

^a The charges are in electrostatic units. C_{CF₃} is the carbon of the CF₃ group; C_{CH₃} is the carbon of the CH₃ group; C_c is the central carbon atom; H_c is the hydrogen bound to the C_c; H_{CH₃} is the hydrogen bound to the CH₃ group. Standard deviation of the charges calculated for different conformers are in parentheses.

were derived from the electronic density obtained from a MP2 calculation using the charges derived by fitting the electrostatic potential (CHELPG) procedure.²⁴ It has been shown that this procedure provides reliable partial charges to use in MD force fields.²⁵ In Table 1, the charges obtained by averaging over the three dominant conformers are reported. The Lennard-Jones (LJ) parameters, excluding the O atom, have been taken from the TFE model⁷ using the GROMOS96¹⁹ force field. The LJ interaction parameters between two different atom types were calculated as the geometric mean of the corresponding LJ parameters of the atom types, as $C_{1,2}^\alpha = \sqrt{C_{1,1}^\alpha C_{2,2}^\alpha}$ with $\alpha = 12$ or 6 and index 1 or 2 referring to the different atom species. Starting from this set of nonbonded interactions, systematic changes of the partial charges of oxygen and hydroxyl hydrogen atoms and the LJ parameters for the O atom were performed. The changes in the LJ oxygen parameters were necessary to reproduce the thermodynamic properties of the liquid solvent. The need to change the oxygen LJ parameters to fit the available experimental data implies that changes in the parameters of HFIP and perhaps TFE would be needed to generate a fully consistent set of models for the three solvents. It also means that no significance should be attributed to slight differences in the radial distribution functions of groups interacting with the oxygen group. Details of simulations are reported in the next section.

2.2. MD Simulations. Different simulations of neat TFIP and mixtures of TFIP with SPC water were performed. A racemic

TABLE 2: A Summary of the Simulations of the Neat Racemic TFIP^a

T (K)	N_{TFIP}	cond ^b	ρ^c	P^d	ΔH_{vap}^e
298	400	<i>NPT</i> (1.4)	1.245	1.0	46.22
298	400	<i>NPT</i> ($\epsilon_{\text{RF}} = 18$)	1.240	1.0	46.25
298	400	<i>NVT</i> (1.4)	1.250	-3.8	46.30
298	400	<i>NVT</i> (1.2)	1.250	102.0	47.00
298	400	<i>NVT</i> (1.4)	1.325	1000.0	48.61
Experiment					
298		<i>NPT</i>	1.250	1.0	44.79

^a The standard deviations of computed values are 5 kg m^{-3} , 300 bar, and 0.4 kJ mol^{-1} for the density, pressure, and vaporization enthalpy, respectively. ^b Cutoff in nm; $\epsilon_{\text{RF}} =$ reaction field. ^c In units of $\text{kg m}^{-3} \times 10^{-3}$. ^d In units of bar. ^e In units of kJ mol^{-1} .

TABLE 3: Thermodynamic Properties of TFIP/Water Mixtures at 298 K under *NPT* Conditions^a

x_{TFIP}	N_{TFIP}	N_{SPC}	ρ^b	P^c	$\Delta H_{\text{mix}}^{\text{calcd } d}$	$\Delta H_{\text{mix}}^{\text{exptl}}$
0.00	0	1074	0.990	1.0		
0.01	20	1876	1.006	1.0	0.24 ± 0.14	-0.08
0.029	50	1680	1.015	0.9	0.21 ± 0.15	-0.15
0.25	200	600	1.05	0.8	1.52 ± 0.33	
0.50	250	250	1.119	0.9	1.97 ± 0.35	
0.60	432	288	1.217	1.0	0.91 ± 0.35	+0.69
0.80	400	100	1.238	0.8	0.69 ± 0.39	+0.50
0.90	400	44	1.240	1.0	0.14 ± 0.48	+0.31
1.00	400	0	1.245	1.0		

^a The standard deviation for the density and the pressure are 5 kg m^{-3} and 300 bar, respectively. The errors in the calculated $\Delta H_{\text{mix}}^{\text{calcd}}$ values are reported directly in the table. ^b In units of $(\text{kg m}^{-3}) \times 10^{-3}$. ^c In units of bar. ^d In units of kJ mol^{-1} .

mixture of TFIP was generated by a direct substitution of the H and F atoms in the CH_3 and CF_3 groups on 50% of the overall number of molecules. All of the simulations of the neat liquid were performed under *NPT* and *NVT* conditions at 298 K. In Table 2, a summary of the simulation parameters is reported. In the case of the mixtures, seven different *NPT* simulations were performed at 298 K. In Table 3, the composition of the mixed systems simulated is reported. The temperature was maintained close to the reference value by weak coupling to an external temperature bath²⁶ with a coupling constant of 0.01 ps (Berendsen thermostat). The pressure was maintained by weak coupling to a reference pressure of $P_0 = 1 \text{ bar}^{26}$ (Berendsen barostat). For the neat liquid, a coupling constant of $\tau_P = 4 \text{ ps}^{26}$ was used. For the mixtures, a coupling constant of $\tau_P = 1 \text{ ps}$ was used. The compressibility of the TFIP was set to the experimental value of $1.22 \times 10^{-4} \text{ bar}^{-1}$.²⁷ Because of the lack of experimental compressibility data for the mixtures with water, the compressibility was set to that of pure water ($4.5 \times 10^{-5} \text{ bar}^{-1}$). The Linear Constrain Solver (LINCS) algorithm²⁸ was used to constrain all bond lengths in TFIP. For the water molecules, the SETTLE algorithm²⁹ was used. A twin range cutoff for the calculation of the nonbonded interactions has been used. All interactions within a short range cutoff of 0.8 nm were updated every step, whereas all interactions (Coulomb and LJ) within a long range cutoff of 1.4 nm were updated only every five steps together with the pair list. The cutoff values are in accord with those standardly used in the GROMOS96 force field.¹⁹ A dielectric permittivity of $\epsilon_r = 1$ and a time step of 2 fs were used. For the simulation performed using the reaction-field correction, the value of the dielectric constant was set to $\epsilon_{\text{RF}} = 18$. Before the simulations were started, the systems were first energy-minimized for 100 steps using the steepest descent algorithm to eliminate unfavorable contacts. Initial velocities were assigned from a Maxwellian distribution corresponding

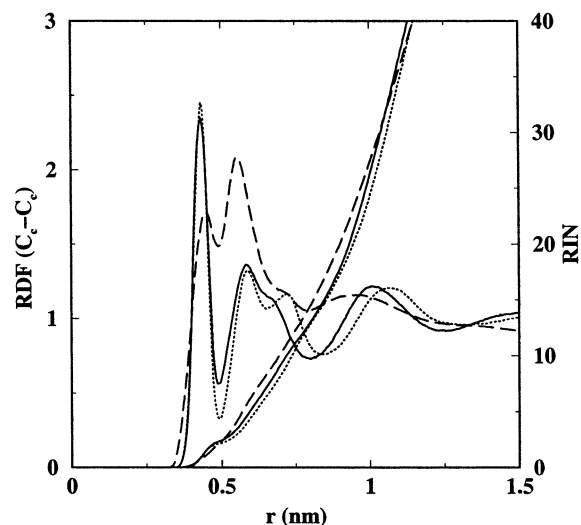


Figure 1. Radial distribution function (RDF) and running integration number (RIN) for the $\text{C}_c\text{-C}_c$ of TFIP (—), TFE (---), and HFIP (···).

to the selected temperature. For the relaxation and equilibration of the systems, simulations of 100 ps long were performed. After equilibration, simulations of 2 ns long were performed for the analysis. Simulations up to 8 ns were also performed to detect possible complete phase separation. All simulations and analysis were performed using the GROMACS package.³⁰

3 Results

3.1. Physicochemical Properties. **3.1.1. Structural Properties.** The intermolecular radial distribution functions (RDFs),³¹ denoted by $g_{xy}(r)$ and calculated from simulations at 298 K, of neat TFIP, TFE, and HFIP are shown in Figure 1. The values for TFE and HFIP were taken from previous studies.^{7,8} In the same figure, the running integration number (RIN),³¹ that is, the average number of atoms y contained in a sphere of radius R centered on atom x , is reported. Only intermolecular contributions to the RDFs are shown. In Figure 1, all of the site-site interactions between the central carbons (C_c) of the three different alcohol molecules have been plotted.

The RDF for the C_c pairs shows a sharp peak at 0.43 nm with a RIN of 1 for both TFIP and HFIP, while for TFE there is a less-defined peak at 0.45 nm with RIN of 1.2. In TFIP, a second and third peak are present at distances of 0.59 and 1 nm with RIN of 4.4 and 26.0, respectively. For HFIP, the peaks are at 0.59 and 1.07 nm with RIN of 4.0 and 24.0, respectively. In TFE only, a second peak is present at 0.55 nm with a RIN of 4.2. The structural similarities between the TFIP and HFIP are clear, the oscillating behavior of the TFIP and HFIP RDFs suggesting that the long-range structural order in both liquids is higher than that of TFE.

Figure 2 shows the O-H RDF for TFIP, TFE, and HFIP. The presence of a hydrogen-bond interaction is evident in all of the liquids indicated in the RDF plots by the sharp peaks at 0.16 nm (RIN of 0.9) for the TFE and HFIP and 0.15 nm (RIN of 1) for the TFIP. This slight difference simply reflects the smaller diameter of the O atom in TFIP. Well-defined second peaks are present for all of the models at 0.29 (TFIP) and 0.32 (TFE, HFIP) with RIN of 2 (TFIP) and 1.7 and 1.8 (TFE and HFIP, respectively). In each of these liquids, the average number of hydrogen bonds in which each molecule is involved is nearly 2 (considering the hydroxy group as both a donor and an acceptor).

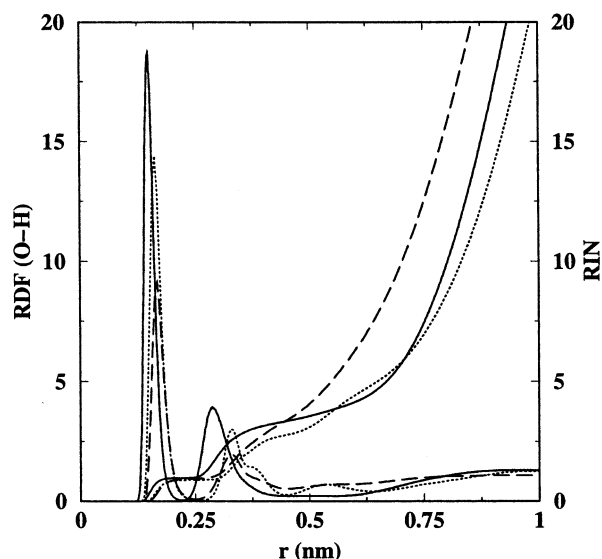


Figure 2. RDF plots and RIN values for the O–H atom pairs: TFIP (—); TFE (---); and HFIP (···).

3.1.2. Thermodynamic Properties. The thermodynamic properties used to optimize the TFIP model were the density,³² pressure, and enthalpy of vaporization¹⁴ at 298 K. The other properties were used as a control. In Table 2, the comparison between the calculated and the experimental values for the density, pressure, and enthalpy of vaporization are reported. The approach used to obtain the enthalpy of vaporization (ΔH_{vap}) and the isothermal compressibility (β_T) was the same as that used previously for the TFE⁷ and HFIP⁸ models. The densities are within 0.4% of the experimental values at 298 K, while the calculated value of β_T , $0.62 \times 10^{-4} \text{ bar}^{-1}$, was less than the experimental value of $1.22 \times 10^{-4} \text{ bar}^{-1}$.²⁷

The simulations discussed in this paper were performed using a long-range cutoff of 1.4 nm for both Lennard-Jones and electrostatic interactions in part because the dielectric constant of TFIP was not available making the inclusion of a reaction-field correction somewhat arbitrary. There are many papers in the literature concerning the relative merits of different schemes to treat in particular long-range electrostatic interactions with arguments for and against the use of lattice sum methods or the introduction of corrections based on a reaction-field approach. In weakly polar systems such as TFIP, the effect of interactions beyond 1.4 nm are negligible. This is shown in Table 2. The dielectric constant of TFIP was estimated to be 18, the average of the dielectric constants of isopropan-2-ol (18.2)³³ and 1,1,1,3,3,3-hexafluoro-2-propanol (17.8).³³ As can be seen, the change in both the density and the heat of vaporization on including a reaction-field correction is less than 0.5%.

3.2. Physicochemical Properties of TFIP, TFE, and HFIP Aqueous Mixtures.

3.2.1. Structural Properties. In Figure 3, the RDFs are plotted for the pairs $O_w\text{--}H$, $O\text{--}H_w$, and $O\text{--}H$ corresponding to a 0.8 molar fraction solution for each of the three solvent models. Note that for all molar fractions other than those at which TFIP and water are not miscible, the general features of the RDFs were largely constant with the RIN number being primarily affected by concentration. A strong hydrogen bond between the water and the alcohols is present, indicated by two well-defined peaks in the RDF for both the $O_w\text{--}H$ (Figure 3a) and $O\text{--}H_w$ (Figure 3b) pairs for all of the solvents. For TFIP, the RDF of the $O_w\text{--}H$ shows a first peak at 0.16 nm with a RIN of 0.7, while for HFIP and TFE the first peak is

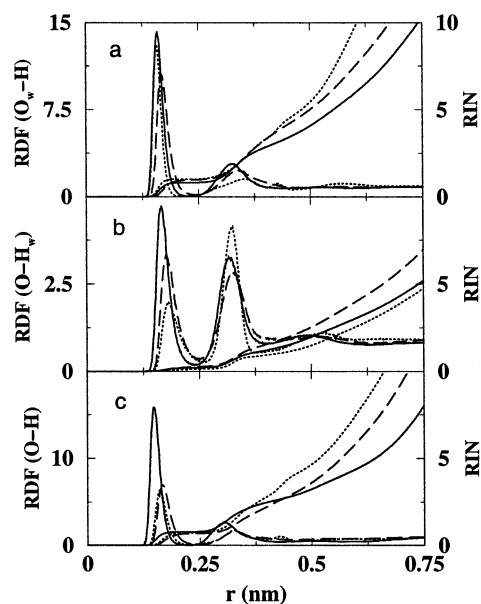


Figure 3. RDF and RIN plots of the (a) hydrogen atom of the TFIP (—), TFE (---), and HFIP (···) with the water oxygen, (b) oxygen atom of TFIP, TFE, and HFIP with the water hydrogen, and (c) intermolecular TFIP, TFE, and HFIP hydrogen bonds in water. All simulations were performed at a molar fraction of $x = 0.8$.

placed at the distance of 0.17 nm with RIN of 0.9, again reflecting differences in the parameters. A second peak is present for all of the liquids with positions of 0.31, 0.33, and 0.35 nm and RINs of 2.6 and 3.0 for TFIP, TFE, and HFIP, respectively. RDFs of the $O\text{--}H_w$ pairs (Figure 3b) show two sharp peaks at 0.165 and 0.32 nm with RIN of 0.2 and 1 for TFIP. For TFE and HFIP, the first and second peak are placed for both at the distance of 0.18 and 0.33 nm with RIN values of 0.68 and 1.2, respectively. The different behavior between the $O_w\text{--}H$ and $O\text{--}H_w$ RDFs for all three solvents can be explained as an effect of the hydrogen-bond acceptor/donor capability of the $O\text{--}H$ atoms. In alcohols with fluorocarbon groups, the basicity of the hydroxy group is reduced and therefore the oxygen atom becomes a weaker H-bond accepting site.^{14,34} In our models, the charge on the O atom is less than that on the oxygen atom of the SPC water model; thus, fluorinated alcohols are weak competitors for the water hydrogen compared to the water itself. The $g_{OH}(r)$ (Figure 3c) denotes a hydrogen bond between the fluorinated alcohol molecules with a sharp maximum at 0.15 nm and a RIN of 0.7 (TFIP) and 0.16 nm with RINs for both TFE and HFIP equal to 0.7. The second peak present at the distance of 0.3 has a RIN equal to 1.3 (TFIP). The second RDF peak for the TFE and HFIP have the values of 0.33 nm (for both) and RINs of 1.2 and 1.7.

3.2.2. Thermodynamic and Kinetic Properties. **3.2.2.1. Hydration Free Energy.** The hydration free energy was estimated using the thermodynamic integration method³⁵ in the same manner as that described previously for the TFE⁷ and HFIP⁸ models. The hydration free energy was calculated by removing a TFIP molecule from a box of 819 SPC water molecules. In this case, the calculation was performed by switching off the nonbonded interactions between the TFIP molecule and the water molecules. The simulations were performed at constant pressure and at 298 K. The calculated free energy of hydration was $-19.3 \pm 3 \text{ kJ mol}^{-1}$ which is in good agreement with the experimental value³⁶ of $-17.4 \text{ kJ mol}^{-1}$.

3.2.2.2. Mixing Enthalpy. In Table 3, the experimental and calculated mixing enthalpies at the different concentrations of

TABLE 4: Calculated (calcd) and Experimental (exptl) Rotational Correlation Times (ps) at 298 K of the CH₃ Group (τ_{CH_3}) and of the TFIP Center of Mass (τ_{C})

x_{TFIP}	$\tau_{\text{CH}_3}^{\text{exptl}}$	$\tau_{\text{CH}_3}^{\text{calcd}}$	$\tau_{\text{C}}^{\text{exptl}}$	$\tau_{\text{C}}^{\text{calcd}}$
0.01	3.8	4.5	5.1	1.1
0.029		4.5		1.2
0.25		4.5		5.0
0.50	4.9	5.5	8.7	6.8
0.60	4.9	4.8	9.0	7.6
0.80	5.1	4.8	10.3	14.7
0.90	6.0	5.2	11.5	15.0
1.00	6.3	5.5	13.7	15.9

TFIP are reported. The calculated values were obtained as described previously for TFE⁷ and HFIP.⁸ From comparison of the calculated mixing enthalpies with the experimental values, it is evident that the agreement is poor for solutions with molar fractions near the miscibility limit of the two liquids and at very low concentrations of TFIP. Probably as for other models of large solvents (more than seven atoms), the poor agreement with the experimental trend could be related to the lack of a specific optimization of TFIP–SPC interactions^{5,37,38} or to the lack of an explicit polarization term in the force field that would affect the intermolecular F \cdots H_w interaction, which plays an important role in the stabilization of the liquid mixtures.^{23,39,40}

3.2.2.3. Rotational Correlation Times. The rotational correlation times (τ_{c}) of the methyl group (τ_{CH_3}) and of the TFIP center of mass (τ_{C}) have been analyzed. All of the τ_{c} were calculated from the correlation function using a second-order Legendre polynomial⁴¹ between two vectors. To determine τ_{CH_3} , vectors were projected through the C_c–C_{CH₃} and C_{CH₃}–H_{CH₃} atom pairs. In the case of τ_{C} , the pairs considered were C_{CH₃}–C_c and C_c–C_{CF₃}. The experimental⁹ and the calculated values are reported in Table 4. The calculated rotational correlation times of the CH₃ group at different molar fractions of TFIP in water are in reasonable agreement with the experimental values. The rotation of the CH₃ group is weakly influenced by the presence of water. In contrast, the rotational correlation times of the whole TFIP around its center of mass are strongly influenced by the concentration of water. The use of the SPC water model, which has a higher diffusion constant and a lower viscosity than that obtained experimentally,⁴² probably accounts for much of the discrepancy between the calculated and experimental values.

4. Discussion

The ΔG_{exp} of hydration of TFE, TFIP, and HFIP are³⁶ –18.02, –17.4, and –15.8 kJ mol^{–1}, respectively. It is evident from these values that the water–alcohol interactions decrease with increasing number of fluorine atoms. This sequence is consistent with a higher hydrophobicity of the CF₃ group compared with the CH₃ group. The presence of alcohol–alcohol interactions results in a different concentration dependence for the three alcohols in water. TFIP has an immiscibility gap between 0.03 and 0.5 molar fraction,^{43,9} while TFE and HFIP are both miscible with water at all concentrations. The low affinity among CH₃ and CF₃ groups in water solution⁹ has been claimed as a possible explanation of the gap in miscibility in TFIP. In fact, the solvation of certain nonpolar solutes in water has been explained by the self-assembly of the solute molecules in solution.⁴⁴

In Figure 4, the RDF between the central carbon atom calculated at different TFIP concentrations is plotted. The curves are compared with that of the pure liquid. The shape of the curves is similar at all concentrations, with the possible exception of the lowest molar fraction ($x = 0.0105$) for which,

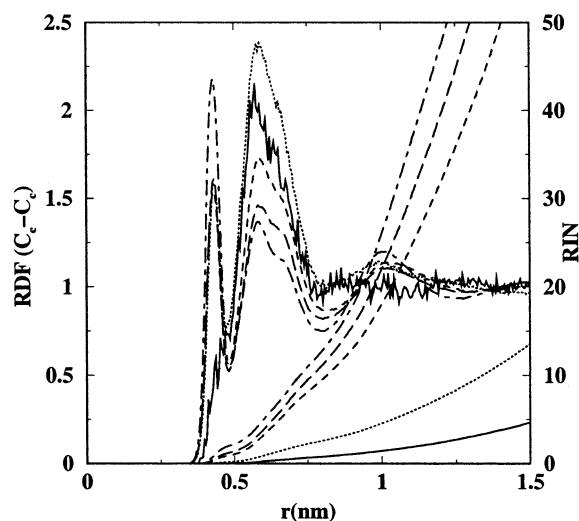


Figure 4. RDF and RIN values between central carbon atoms of the TFIP molecules in water solutions at different molar fractions, x : (—) $x_{\text{TFIP}} = 0.0105$; (···) $x_{\text{TFIP}} = 0.029$; (---) $x_{\text{TFIP}} = 0.25$, (- · - ·) $x_{\text{TFIP}} = 0.5$; (- - -) $x_{\text{TFIP}} = 0.9$.

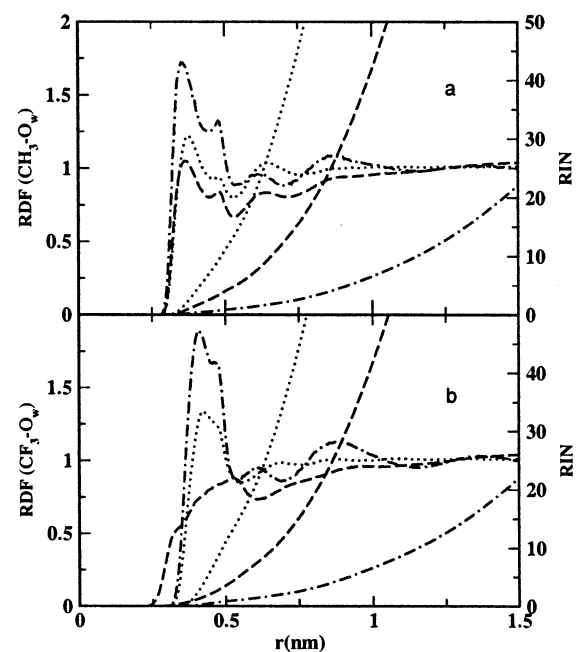


Figure 5. RDF and RIN plots of (a) the methyl group with the water oxygen (b) the trifluoromethyl group with water oxygen: (···) $x_{\text{TFIP}} = 0.029$; (---) $x_{\text{TFIP}} = 0.5$; (- · - ·) $x_{\text{TFIP}} = 0.8$.

because of a lack of statistics, the curve is less smooth. The slight changes in the position of the first peak in the RDF reflect the influence of water on the aggregation of TFIP. At higher TFIP concentrations, the RDF becomes similar to that of the pure liquid. The RIN, calculated at distance of 1 nm, increases with the concentration from 1.0 at $x = 0.0105$ to 25.5 at $x = 0.9$. The corresponding value for the pure liquid is 26.0.

In Figure 5, RDFs of the CH₃ and CF₃ groups with respect to the water oxygen are plotted. The distribution of water around the methyl group (Figure 5a) is similar to that observed for methane in water.⁴⁵ It is also evident that the main features of this plot are independent of the TFIP concentration. In contrast, the water structure around the CF₃ group varies markedly with the concentration of TFIP (Figure 5b). At low TFIP concentration ($x = 0.029$), the water around the CH₃ group is ordered. Surrounding the CF₃ group, there is also an ordered shell of

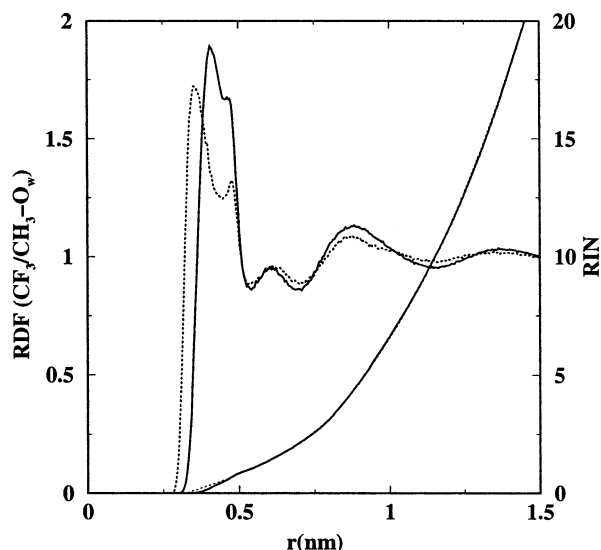


Figure 6. RDF and RIN plots of the methyl group (···) and the trifluoromethyl group (—) with the water oxygen at 0.8 molar fraction of TFIP.

water although the broader peaks indicate that it is slightly less well-defined. Increasing the concentration of TFIP to $x = 0.5$ results in a loss of order of the water shell around the CF_3 group with very broad peaks. Interestingly, at a molar fraction of $x = 0.8$, the water cage around the CF_3 group is again restored. These data are consistent with the existence of an incompatibility in the solvation structure of the CF_3 and CH_3 .¹⁴ To investigate a possible difference between the solvation shells for the CF_3 and CH_3 groups at concentrations where TFIP and water are miscible, the RDFs for the CF_3 and CH_3 groups with the water oxygen at a molar fraction of $x = 0.8$ are reported (Figure 6). The RDF has the same maxima and minima in the second shell with a shift of the first peak due to the different dimensions of the two groups. This indicates a similar organization of water molecules in the shell surrounding the two groups. Also in aqueous mixtures TFE and HFIP (data not shown), the solvation structure of the first solvation is independent of the alcohol concentration. The effect of the solvation shell becomes evident if we analyze the RDF for the CH_3 – CF_3 pairs. In Figure 7, the RDFs for the CH_3 and CF_3 pairs at three different concentrations are reported and compared with that of the neat liquid. Even at very low concentrations of TFIP, the shape of the function is similar to that of the neat liquid with no shifts of the peak positions. This confirms that the interaction with water does not disturb the geometrical arrangements of the TFIP molecules.

Experimentally, the rotational correlation times⁹ of HFIP and TFIP are low in comparison to 2-propanol, indicating that the intermolecular hydrogen bonds with water are stronger. The TFIP hydroxyl group seems to interact with water in a similar way as that for the hydroxyl group in HFIP. This means that the phase separation observed in TFIP/water mixtures can be attributed to the interaction of hydrophobic groups, as opposed to the hydroxyl group. In the simulations, a complete separation of TFIP and water was not observed at any molar fraction (see Figure 4).

In this regard, the model does not reproduce the expected macroscopic properties of the TFIP–water mixtures. Phase separation is a collective property of a system. It is thus far from certain whether phase separation should be observed on the microscopic length and time scales simulated. In this regard, a distinction must be made between the behavior of, for example, hexane, which is immiscible in water except at

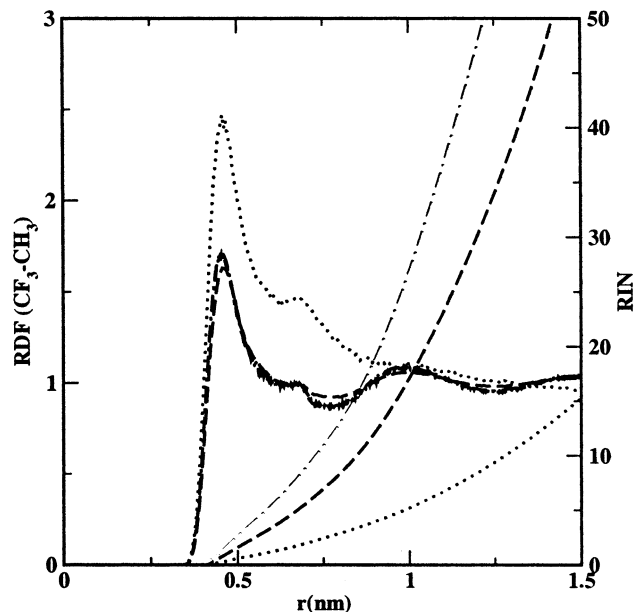


Figure 7. RDF and RIN of the methyl–trifluoromethyl groups at (···) $x_{\text{TFIP}} = 0.029$, (---) $x_{\text{TFIP}} = 0.5$, and (-·-·) $x_{\text{TFIP}} = 0.8$.

extremes of concentration and which readily phase separates in simulations, and the expected behavior of TFIP, which is miscible at most concentrations. In the case of TFIP, separate phases are only thermodynamically stable in a narrow concentration range and presumably as a collective effect in a macroscopic volume. What we do observe in the simulations is a marked change in structure suggesting that the system cannot pack efficiently at molar ratios at which phase separation occurs. The simulations thus provide a microscopic interpretation of a possible origin for phase separation in macroscopic systems.

Nevertheless, the calculated τ_C were in good agreement with the experimental values and yield the same overall trend. Instead of a complete phase separation, the effect of different concentrations of TFIP is reflected in the different organization of the water shells around the CH_3 and CF_3 groups.

5. Conclusions

We have used molecular dynamics simulation techniques to analyze the unusual thermodynamic behavior of TFIP and to investigate the nature of the CF_3 –water interaction. The investigation was performed using a new model for racemic TFIP suitable for MD simulations. The model was parametrized to reproduce the heat of vaporization and the experimental density at standard pressure of the neat liquid and is compatible with the GROMOS96 force field. The calculated thermodynamic properties of the model show satisfactory agreement with the experimental data. The TFIP model was then used in combination with the SPC water model to analyze the structural, thermodynamic, and kinetic properties of a range of aqueous mixtures. The simulations suggest that the structure of the solvent around the CF_3 group is central to understanding why TFIP is only miscible with water at certain concentrations. The shell of solvating water is poorly structured around the trifluoromethyl group at concentrations at which TFIP and water are immiscible (between 0.03 and 0.5 molar fractions). In contrast, at concentrations at which the two liquids are miscible, the water solvation shell around the CF_3 group is well structured and similar to that surrounding the CH_3 group. The solvation shell around the CH_3 group is always similar to that of methane in water.⁴⁵ Changes in the structure of the water around the CF_3

group may explain the high enthalpy of mixing of this compound calculated between $0.03 < x < 0.5$ molar fraction of TFIP. For TFE or HFIP, the observed miscibility with water may be explained by the fact that these alcohols cluster strongly in water, giving a microheterogeneous solution on a molecular scale.^{7,8,46} In the case of the TFIP, clustering is less pronounced in part because of a failure of the CH₃ and CF₃ groups to interact strongly. This may oblige the different hydrophobic groups to be exposed to the water (with a high enthalpic/entropic cost). This inability to reduce the exposure of hydrophobic surface area by clustering may explain the sharp transition from miscible to immiscible at certain molar fractions of TFIP and water.

Acknowledgment. M. Fioroni is grateful to the EC for the TMR project "Fluorine: a Unique Tool for Engineering Molecular Properties" [Grant ERBFMRXCT 970120] to the Vigoni project and to Prof. D. Vogt for his help. D. Roccatano thanks the Italian Ministero dell'Istruzione, Università e Ricerca (National project "Structural Biology and Dynamics of redox proteins").

References and Notes

- (1) Degrado, W.; Summa, C.; Pavone, V.; Natri, F.; Lombardi, A. *Annu. Rev. Biochem.* **1999**, *68*, 779–819.
- (2) Giver, L.; Gershenson, A.; Freskgard, P.; Arnold, F. *Proc. Natl. Acad. Sci. U.S.A.* **1995**, *95*, 12809–12813.
- (3) Osipov, S.; Burger, K. *Tetrahedron Lett.* **2000**, *41*, 5659–5662.
- (4) Leo, A. *Chem. Rev.* **1993**, *93*, 1281–1306.
- (5) Muller, N. *J. Pharm. Sci.* **1986**, *75*, 987–991.
- (6) Dong-Pyo, H.; Masaru, H.; Ryoichi, K.; Yuji, G. *J. Am. Chem. Soc.* **1999**, *121*, 8427–8433.
- (7) Fioroni, M.; Burger, K.; Mark, A. E.; Roccatano, D. *J. Phys. Chem. B* **2000**, *104*, 12347–12354.
- (8) Fioroni, M.; Burger, K.; Mark, A. E.; Roccatano, D. *J. Phys. Chem. B* **2001**, *105*, 10967–10975.
- (9) Mizutani, Y.; Kamogawa, K.; Kitagawa, T.; Shimizu, A.; Taniguchi, Y.; Nakanishi, K. *J. Phys. Chem.* **1991**, *95*, 1790–1794.
- (10) Hildebrand, J. H.; Prausnitz, J. M.; Scott, R. L. *Regular and Related Solutions*; Van Nostrand-Reinhold: New York, 1970.
- (11) Mukerjee, P.; Young, A. Y. S. *J. Phys. Chem.* **1976**, *80*, 1388–1390.
- (12) Carlfors, J.; Stilbs, P. *J. Phys. Chem.* **1984**, *88*, 4410–4414.
- (13) Kim, N.; Shin, S. *J. Chem. Phys.* **1999**, *110*, 10239–10242.
- (14) Rochester, H.; Symonds, J. R. *J. Chem. Soc., Faraday Trans. I* **1973**, *69*, 1267–1273.
- (15) Kamogawa, K.; Kitagawa, T. *Vibrational Spectra and Structure*; Elsevier: Amsterdam, 1989; Vol. 17B.
- (16) VanBuuren, A. R.; Berendsen, H. J. C. *Biopolymers* **1993**, *33*, 1159–1166.
- (17) Gough, C. A.; DeBolt, S. E.; Kollmann, P. A. *J. Comput. Chem.* **1992**, *13*, 963–970.
- (18) Kinugawa, K.; Nakanishi, K. *J. Chem. Phys.* **1988**, *89*, 5834–5842.
- (19) van Gunsteren, W. F.; Billeter, S. R.; Eising, A. A.; Hünenberger, P. H.; Krüger, P.; Mark, A. E.; Scott, W. R. P.; Tironi, I. G. *Biomolecular Simulation: The GROMOS96 Manual and User Guide*; vdf Hochschulverlag: ETH Zürich, Switzerland, 1996.
- (20) Berendsen, H. J. C.; Postma, J. P. M.; van Gunsteren, W. F.; Hermans, J. *Interaction Models for Water in Relation to Protein Hydration. In Intermolecular Forces*; Pullmann, B., Ed.; Reidel: Dordrecht, Netherlands, 1981; pp 331–342.
- (21) Frisch, M. J.; Trucks, G. W.; Schlegel, H. B.; Scuseria, G. E.; Robb, M. A.; Cheeseman, J. R.; Zakrzewski, V. G.; Montgomery, J. A., Jr.; Stratmann, R. E.; Burant, J. C.; Dapprich, S.; Millam, J. M.; Daniels, A. D.; Kudin, K. N.; Strain, M. C.; Farkas, O.; Tomasi, J.; Barone, V.; Cossi, M.; Cammi, R.; Mennucci, B.; Pomelli, C.; Adamo, C.; Clifford, S.; Ochterski, J.; Petersson, G. A.; Ayala, P. Y.; Cui, Q.; Morokuma, K.; Malick, D. K.; Rabuck, A. D.; Raghavachari, K.; Foresman, J. B.; Cioslowski, J.; Ortiz, J. V.; Stefanov, B. B.; Liu, G.; Liashenko, A.; Piskorz, P.; Komaromi, I.; Gomperts, R.; Martin, R. L.; Fox, D. J.; Keith, T.; Al-Laham, M. A.; Peng, C. Y.; Nanayakkara, A.; Gonzalez, C.; Challacombe, M.; Gill, P. M. W.; Johnson, B. G.; Chen, W.; Wong, M. W.; Andres, J. L.; Head-Gordon, M.; Replogle, E. S.; Pople, J. A. *Gaussian 98*, revision A.3; Gaussian, Inc.: Pittsburgh, PA, 1998.
- (22) Marstokk, K. M.; Mollendall, H. *Acta Chem. Scand.* **1998**, *52*, 1307–1312.
- (23) Schaal, H.; Häber, T.; Suhm, M. A. *J. Phys. Chem. A* **2000**, *104*, 265–274.
- (24) Breneman, C. M.; Wiberg, K. B. *J. Comput. Chem.* **1990**, *11*, 361–397.
- (25) Carlson, H. A.; Nguyen, T. B.; Orozco, M.; Jorgensen, W. J. *Comput. Chem.* **1993**, *14*, 1240–1249.
- (26) Berendsen, H. J. C.; Postma, J. P. M.; DiNola, A.; Haak, J. R. *J. Chem. Phys.* **1984**, *81*, 3684–3690.
- (27) Mehta, S. K.; Sharma, A. K.; Parkash, R.; Chadha, S. L. *J. Chem. Soc., Faraday Trans.* **1998**, *94*, 2565–2569.
- (28) Hess, B.; Bekker, H.; Berendsen, H. J. C.; Fraaije, J. G. E. M. *J. Comput. Chem.* **1997**, *18*, 1463–1472.
- (29) Miyamoto, S.; Kollman, P. A. *J. Comput. Chem.* **1992**, *13*, 952–962.
- (30) van der Spoel, D.; Berendsen, H. J. C.; van Buuren, A. R.; Apol, E.; Meulenhoff, P. J.; Sijbers, A. L. T. M.; van Drunen, R. *Gromacs User Manual*; 1995.
- (31) Allen, M. P.; Tildesley, D. J. *Computer Simulations of Liquids*; Oxford Science Publications: Oxford, U.K., 1987.
- (32) Evans, A.; McElroy, G. *J. Solution Chem.* **1975**, *4*, 413–416.
- (33) *Tabellenbuch Chemie*; VEB Deutscher Verlag für Grundstoffe Industrie: Leipzig, Germany, 1980.
- (34) Chambers, D. *Fluorine in Organic Chemistry*; John Wiley & Sons: Chichester, U.K.–New York, U.S.A., 1973.
- (35) Mark, A. E. Free Energy Perturbation Calculations. In *Encyclopedia of Computational Chemistry 2*; von Rague Schleyer, P., Ed.; John Wiley & Sons: New York, 1998; pp 1070–1083.
- (36) Cabani, S.; Gianni, P.; Mollica, V.; Lepori, L. *J. Solution Chem.* **1981**, *10*, 563–595.
- (37) Chitra, R.; Smith, P. E. *J. Chem. Phys.* **2001**, *114*, 426–435.
- (38) Chitra, R.; Smith, P. E. *J. Phys. Chem. B* **2000**, *104*, 5854–5864.
- (39) Alkorta, I.; Rozas, I.; Elguero, J. *J. Fluorine Chem.* **2000**, *101*, 233–238.
- (40) Erickson, J. A.; McLoughlin, J. I. *J. Org. Chem.* **1995**, *60*, 1626–1631.
- (41) Tironi, I. G.; van Gunsteren, W. F. *Mol. Phys.* **1994**, *83*, 381–403.
- (42) van der Spoel, D.; van Maaren, P. J.; Berendsen, H. J. C. *J. Chem. Phys.* **1998**, *108*, 10220–10230.
- (43) Mitsuhiro, D.; Touhara, H.; Nakanishi, K. *J. Chem. Thermodyn.* **1987**, *119*, 539–542.
- (44) Marmur, A. *J. Am. Chem. Soc.* **2000**, *122*, 2120–2121.
- (45) Cui, Q.; Smith, V. H., Jr. *J. Chem. Phys.* **2000**, *113*, 10240–10245.
- (46) Chitra, R.; Smith, P. E. *J. Chem. Phys.* **2001**, *115*, 5521–5530.